Energy & Environmental Science

Accepted Manuscript

This article can be cited before page numbers have been issued, to do this please use: K. Han, J. Luo, Y. Feng, L. Xu, W. Tang and Z. Wang, *Energy Environ. Sci.*, 2020, DOI: 10.1039/D0EE01102A.

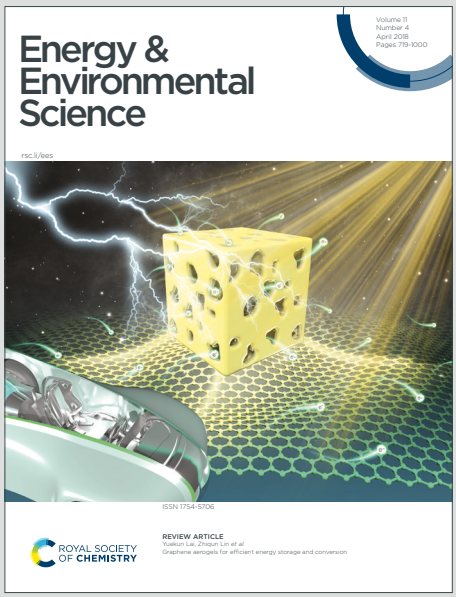

ROYAL SOCIETY OF CHEMISTRY

rsc.li/ees

View Article Online
DOI: 10.1039/D0EE01102A

ARTICLE

Self-Powered Electrocatalytic Ammonia Synthesis Directly from Air as Driven by Dual Triboelectric Nanogenerators

Received 00th January 20xx,
Accepted 00th January 20xx

DOI: 10.1039/x0xx00000x

Kai Han,[ab] Jianjun Luo,[ab] Yawei Feng,[ab] Liang Xu,[abc] Wei Tang *[abc] and Zhong Lin Wang* [abd]

Electrocatalytic reduction at room temperature and atmospheric pressure is a promising low-power-consumption and eco-friendly pathway to replace traditional ammonia synthetic methods, which is one of the largest chemical processes in terms of energy consumption and greenhouse gas emissions. In this work, we utilize triboelectric nanogenerator (TENG) to construct an electrocatalytic ammonia synthesis system with air as nitrogen source, which is self-powered, eco-friendly, low-cost, facile-fabrication, and scalable. The nitrogen fixation and electrocatalytic reduction can proceed simultaneously by introducing a high-output dual-TENG configuration. A needle-plate structure is utilized to achieve air discharge and thus obtain NO_x for further aqueous electrolyte formation. In addition, an electrochemical cell with TiO_2 as the catalyst is used to synthesize ammonia. Driven by the simulated waste gas at a flow rate of 3.5 m^3 min^{-1}, ammonia yield per hour of the self-powered electrocatalytic system reaches 2.4 μg h^{-1}.

Introduction

As one of the largest inorganic productions in the world, ammonia has played an important role in fertilizer making and other chemicals producing.[1] Correspondingly, ammonia synthesis consumes huge quantities of fossil fuels. Besides, represented by Haber–Bosch process, traditional synthetic methods require hash conditions such as high temperature and high pressure, which increases the demand for energy and the harm to environment.[2] Therefore, searching for low-power-consumption and eco-friendly methods is urgent. Electrochemical reduction at room temperature and atmospheric pressure especially in aqueous electrolyte is a promising pathway to achieve this.[3, 4]

Since it is a great challenge to break the stable nitrogen-nitrogen triple bond due to its high bond energy (940.95 kJ mol^{-1}) under ambient conditions,[5] present studies focus more on electrocatalysts for the reduction of N_2 to ammonia. Recently, various materials from noble metals (Pd, Au etc.), normal metals and metallic compounds (Cu, TiO_2, MoS_2 etc.) to non-metallic materials (black phosphorus, COF etc.) are utilized and show a good electrocatalytic performance under a constant electric drive (Table S1). Zhang et. al.[6] used black phosphorus nanosheets as an efficient non-metallic catalyst, which achieved a high NH_3 yield of 31.37 μg h^{-1} $mg^{-1}_{cat.}$ at -0.7 V vs. reversible hydrogen electrode (RHE). By defect-rich MoS_2, another work by Li et. al.[7] also shows outstanding performance with a yield of 29.28 μg h^{-1} $mg^{-1}_{cat.}$ at -0.40 V vs. RHE. However, for a new catalyst, there are varied sources of potential experimental artefacts need to be dealt for reliable proof, such as interferences from labile nitrogen-containing compounds, even the catalyst itself in the system.[8-10] In addition, in order to avoid the influence of oxygen and increase the amount of nitrogen in the electrolyte, the requirement for high purity nitrogen source is another issue.[11,12] Though some researchers tried using air or wet air for the ammonia synthesis, additional heating is usually needed in these systems, even over 400 °C (Table S1). Apart from electrocatalytic N_2 reduction, other nitrogen-rich compounds nitrate and nitrite are utilized to be reduced into ammonia in the view of wastewater treatment.[13,14] Nevertheless, because of the complex composition of wastewater, there will be a series of intractable problems from selective catalysis to later extraction. Thus, it is significant to seek other ways to realize bond breaking and following synthesis from the perspective of energy, catalytic reduction and process controllability.

Originating from Maxwell's displacement current, the triboelectric nanogenerator (TENG) is a developing technology in energy harvesting with huge practical value.[15-18] Based on a series of advantages such as wide material sources and simple fabrication, various TENGs have been utilized to convert multiform mechanical energy into electric energy for different applications,[18-23] including self-powered electrochemical reaction.[24-26] Besides, due to the high voltage property of TENG, it can easily build a strong electric field to realize the chemical bond breaking, including nitrogen fixation.[27,28] Furthermore, since billions of tons of flue gas is exhausted into

[a] CAS Center for Excellence in Nanoscience, Beijing Institute of Nanoenergy and Nanosystems, Chinese Academy of Sciences, Beijing 100083, P. R. China Email: tangwei@binn.cas.cn
[b] School of Nanoscience and Technology, University of Chinese Academy of Sciences, Beijing 100049, P. R. China
[c] Center on Nanoenergy Research, School of Physical Science and Technology, Guangxi University, Nanning 530004, P.R. China
[d] School of Material Science and Engineering, Georgia Institute of Technology, Atlanta, Georgia 30332-0245, USA. Email: zlwang@gatech.edu
† Electronic Supplementary Information (ESI) available. See DOI: 10.1039/x0xx00000x

DOI: 10.1039/D0EE01102A

the air every year,[29] it will be celebrating by using the residual gas kinetic energy for self-powered synthesis before emission.

In this work, taking the high-voltage advantage of the TENG, the nitrogen fixtation is simply realized by directly using air as source, distinguished from electrocatalytic N_2 reduction. In addition, the self-powered characteristics of the TNEG leads to a non-noble-metal electrocatalytic reduction, in which no extra electrolyte addition and no power are needed. Sepecically, by using air discharge induced by the high voltage from the TENG, nitrogen and oxygen are ionized and fixed into NO_X. Then the gas flow with NO_X is washed by water and directly forms electrolyte contains NO_3^- and NO_2^- for further reaction. Additionally, driven by the other simultaneously working TENG, electrocatalytic reduction is carried out to synthesize ammonia in an electrochemical cell. Furthermore, all of these can be simply achieved by the power of simulated waste gas at room temperature and atmosphere pressure.

Results and Discussion

Fig. 1a shows a structure diagram of the dual-TENG device for self-powered ammonia synthesis. Two disk-structure TENGs in non-contact-sliding freestanding mode are assembled vertically with a common drive shaft. The stator is a PCB circuit board with 6 pairs of Cu electrodes in parallel connection, which is fixed on an aluminum plate. The rotor is composed of 6 separate Kapton films on a substrate of epoxy glass cloth board (FR-4). In order to reduce rotational inertia for less energy consumption and sufficient mechanical strength, a thickness of 0.3 mm of FR-4 is selected. Before the device is assembled, the Kapton film is initially negatively charged by rubbing with the Cu film. It is noted that there is a small gap between the rotor and the stator to reduce friction resistance for high-speed rotation. The power generation principle of non-contact-sliding freestanding mode TENG in short-circuit state is shown in Fig. 1b. Two pairs of electrodes are drawn to help describe the mechanism. Since the Kapton film is negatively precharged, positive charges are induced in the electrode right below. In the first half cycle of electricity generation, as the rotor slides, the positive charges will flow from the first electrode to the next in the circuit until the Kapton reaches the overlapping position of next electrode. As the sliding continues, the induced positive charges will keep flowing to the next electrode in the same way. Since the electrodes are connected in parallel, the current direction is reverse in the circuit. When the first Kapton film is on the overlapping position of first electrode in the second pair, a complete cycle of electricity generation process is over. The devices and corresponding main reaction processes and mechanism are illustrated in Fig. 1c. In order to break the strong nitrogen-nitrogen bond, a typical discharge device with a needle-plate structure is employed. Besides, a ten-stage voltage multiplier circuit is connected to TENG-1 to achieve a higher voltage. As TENG-1 works, strong electric field is generated and able to excite and ionize nitrogen and oxygen molecules in the space between needle and plate. The discharge process is an important step to fix nitrogen and produce NO_X.[30,31] The air is continuously flowed through the device and then be inlet into a gas-washing bottle with water in it, thus producing electrolyte containing NO_3^- and NO_2^-. Meanwhile, with circuit management by a transformer and a rectifier, TENG-2 can be simply viewed as a pulsed DC power to drive the following electrocatalytic reduction for ammonia synthesis. As for the cathode region, NO_3^- can be reduced into NH_3 directly or NO_2^- first. The new produced and pre-existing NO_2^- can be further reduced into NH_3. As for the anode region, oxygen is a main product of oxidation of water.

Tested by an electrometer and a multimeter with high-voltage attenuation, the basic performance of dual-TENG device is shown in Fig. 2. A high-speed motor with a controller is used as the simulated driving force. As shown in Fig. 2a-f, both TENG-1 and TENG-2 show high output performance with no significant difference. With the increase of motor speed, the transferred charge and short-circuit current gradually become larger and reach to about 1 μC and 0.55 mA at a speed of 5000 r min^{-1} respectively. Meanwhile, the open-circuit voltage of both TENGs remains relatively stable in a range of 630-720 V. It is worth noting that there should be no speed dependency for the transferred charge based on the fundamental theory of sliding freestanding TENG.[17] Since the ratio of thickness to diameter of FR-4 substrate is 0.15%, it is hard to keep it horizontal all the time. Thus, there will be unwanted frictions with Cu electrodes, especially at low rotation speed. The positive charge generated on FR-4 will weaken the induced electric field and reduce transferred charge. As the speed rises, such negative effect will reduce with fewer frictions. In addition, the maximum peak power is examined as well and shown in Fig. S1.

Although the TENGs have shown a good high-voltage characteristic, a ten-stage voltage multiplier circuit containg capacitors and diodes is utilized to obtain higher voltage for better air discharge performance.[32-34]The basic working priciple of this circuit is shown in Fig. S2, and more detailed information is described in the Electronic Supplementary information.Four kinds of high-voltage resistive capacitors with same diodes are assembled and tested with TENG-1, respectively. As shown in Fig. 3a, a 50 nF capacity is better to help boost the voltage to an expected value about 7 kV. It is inferred that a low capacity could not be able to store too much charge, which may lead to electric leakage and reduce the boost effect. A typical discharge structure is utilized (Fig. 3b), in which contains a steel needle and a Tantalum sheet as electrodes. Tantalum is a kind of corrosion-resistant metal with non-noble property, which is a good choice for acid gas environment containing NO_X. Since the multiplier circuit has the AC to DC conversion capability, the needle is used as positive or negative electrode to explore which condition is better for NO_X production. According to Paschen's law, the distance between the tip of needle and the bottom plate electrode is set as a control variable at atmospheric pressure. The concentration variation of NOx is illustrated in Fig. 3c and 3d, which is recorded after 5 min discharge. The distances of 3 mm and 2 mm are the respective optimal parameters for positive and negative conditions. When the distance becomes bigger than the optimal value the concentration decreases, which is attributed to the weaker electric field and following less ionization in corona

View Article Online
DOI: 10.1039/D0EE01103A

discharge. As for the shorter distance, the production of NO_X is much less. It is infered that the obvious hard light from impulse spark discharge (Fig. 3e) which consumes a lot of energy may be an important reason. The distance conditions of pictures (i) and (ii) have a good correpond to the results in the pink dotted box of Fig. 3c. And the distance condition of pictures (iii) has a good correpond to the result in the blue dotted box of Fig. 3d. In addition, it is observed that more NO_X products are detected when the needle used as the negative electrode. It is inferred that strong electric fields in different directions cause different ionizations.[35] Since what we need is electrolyte for ammonia synthesis, the concentration in solution is more meaningful. Then, the discharge device with a needle-plate distance of 2 mm is sealed in another smaller box with air inlet and outlet. Air flow through the device brings the generated NOx into a gas-washing bottle with 20 mL pure water. After 6 h discharge, the concentrations of NO_3^- and NO_2^- are determined (Fig. 3f and 3g) according to their standard curves (Fig. S3). When at a positive electrode state, NO_3^- and NO_2^- are in a same concentration level less than 1 mg L^{-1}. As for a negative electrode state, the concentration of NO_3^- is much higher and achieves 7.4 mg L^{-1} while the concentration of NO_2^- is less than 0.02 mg L^{-1}. Since the air flow will take some water molecules away, the residual volume is measured after each discharge as well (Fig. S4). The yield per hour data are shown in Fig. 3g and 3h to have a better comparison. Based on the results above, a condition of using needle as a negative electrode with a needle-plate distance of 2 mm is selected.

As an effective, cheap and low toxic catalyst, TiO_2 is widely used in photocatalytic and electrocatalytic reactions, in which reductions of nitrate and nitrite are involved as well.[36-39] Herein, a kind of commercial nano-TiO_2 (P25) is introduced into the electrocatalytic system for ammonia synthesis. In a single cell, a carbon cloth covered by TiO_2 nano particles is used as the working electrode, a graphite electrode is used as the counter electrode. As a comparison, naked carbon cloth is also used for electrochemical reduction. Fig. 4a and 4b show the SEM images of carbon cloth and TiO_2/carbon cloth under different magnification. Since the main electrolyte forms in solution are NO_3^- and NO_2^- from air discharge, KNO_3 and KNO_2 are chosen as the simulation reactant separately to verify the feasibility for ammonia synthesis. The cyclic voltammetry (CV) curve is measured in a 20 mL of 100 mg L^{-1} NO_3^- or NO_2^- solution with the reference of saturated calomel electrode (SCE) (Fig. S5). There are distinguishable differences when TiO_2 is added. Using NO_3^- solution as the primary electrolyte, the electrocatalytic reduction results driven by a DC power at -3 V for 6 h are shown in Fig. 4c and Fig. S6. According to the standard curve (Fig. S7), the concentration of target product NH_3 is higher when using TiO_2. Besides, as an intermediate product or by-product of reduction, the concentration of NO_2^- is much lower when TiO_2 exists, which stands for a better catalytic selectivity and efficiency. When directly using NO_2^- solution as the electrolyte, the results also show a better reduction for ammonia (Fig. S8). Furthermore, another verification test using NO_3^- electrolyte at a constant current condition with -0.25 mA by an electrochemical workstation is conducted as well, in which a same trend and catalytic performance are shown (Fig. S9). Then, the electrocatalytic system with TiO_2 is applied in the following experiments. At a rotation speed of 5000 r min^{-1}, it is clear to see that ammonia is synthesized successfully driven by TENG-2 after rectification for 6 h (Fig. 4d). The concentrations of NO_3^- and NO_2^- are also determined and shown in Fig. S10. To get more ammonia production, an electromagnetic transformer is introduced to get a higher current output for a better reduction.[25] Thus, the voltage and the current variations with different concentrations of NO_3^- and different transformer ratios are tested. In general, once the voltage could satisfy the condition to drive the reaction, a larger current is better for synthesis. As shown in Fig. S11, the optimal transformer ratio has a migration trend from small to large with the increase of NO_3^- concentration. Then, a transformer ratio of 350:12 is selected to verify its effect. Fig. 4e shows that more ammonia is synthesized with the help of a transformer. A simple comparison of ammonia yield by different powers is shown in Fig. S12. With the drive of TENG, a comparable yield to DC power can be got. Besides, it is clear to see that the yield achieves 20.8 μg h^{-1} with transformer, which is about 3.5 times that of without. Furthermore, a comparison of Faraday efficiency is shown in Fig. S13 as well. More information about the calculation is illustrated in the Electronic Supplementary Information. The efficiency by TENG-2 is 13.9%, which is about half value by DC power. However, it is still comparable, showing a good application potential. Here, it is significant to note that there is a severe anodic corrosion with the current up to a milliampere level (Fig. S14a) when using a transformer. Such corrosion will cause electrolyte pollution and strong interference to the detection and further purification. After dilution, there is much less influence on the determination of NO_2^- and NH_3. However, strong interference of absorption in ultraviolet region still exists (Fig. S14b). Therefore, a dual-compartment electrochemical cell with a fuel cell structure is introduced (Fig. 4f). The cell is assembled by graphite bipolar plate, silicone seal, nafion membrane (NRE-211) and TiO_2/carbon cloth. Pictures of main components are shown in Fig. S15. The dual-compartment electrocatalytic cell is driven by the rectified TENG-2 at a rotation speed of 5000 r min^{-1}. A 20 mL of pure water and a 20 mL of 100 mg L^{-1} NO_3^- solution are recycled in the anode region and cathode region separately for 1 h reaction by two peristaltic pumps both at a rate of 1 mL min^{-1}. Before the sustained reaction, the selection process for a suitable transformer is conducted as well (Fig. S16) and a ratio of 350:4 is used. After 1 h reaction, the determination results of anode and cathode compartments are shown in Fig. 4g. The ammonia yield per hour in the cathode area is 27.5 μg h^{-1}, which is a little higher than the reaction in a single cell. Besides, a continuous reaction for 6 h with determination every hour is tested and the result is clearly shown in Fig. S17.

Taking advantage of TENG, it is feasible to reuse the residual kinetic energy of billions of tons of exhaust gas from factories to supply mechanical energy, and meanwhile carry out in-situ ammonia synthesis for factories, which is energy-saving and eco-friendly. As shown in Fig. 5a, with the help of a turbocharger, the gas flow will rotate the turbofan and shaft to

make TENG produce electric energy and be recollected for emission. Based on the above, a dual-compartment electrochemical cell with TiO_2 as the catalyst and a previously mentioned discharge device are utilized to construct a self-powered system with TENGs. The gas-washing bottle is directly connected to the cathode compartment to supply electrolyte. To avoid the determination interference from ammonia in the air, two gas filters both with 30 mL of 0.05 M H_2SO_4 are set ahead of the discharge device. A blower is used as the simulated exhaust gas source and combined with the dual-TENG and a commercial turbocharger to drive the system for ammonia synthesis (Fig. 5b). The whole system is set at a work condition of gas flow rate of 3.5 m^3 min^{-1}. Basic performance of the dual-TENG and other relevant information of the system at the initial stage of reaction are tested. After calculation, the rotation speed is about 2000 r min^{-1}. In addition, the best transformer ratio is chosen as 350:5 (Fig. S18). Fig. 5c shows the open-circuit voltage and ten-stage multiplied voltage of TENG-1. Open-circuit voltage and short-circuit current of TENG-2 are illustrated in Fig. 5d and 5e. After voltage step-down and rectification, TENG-2 outputs voltage and current for the dual-compartment electrocatalytic cell around 3.1V and 8.9 mA respectively. After 10 h reaction, NH_3 is synthesized successfully by the self-powered system. The determination result is clearly shown in Fig. 5f. By measuring the solution volume involved in the cathode reaction (Fig. 5g), the self-powered ammonia yield per hour achieves 2.4 μg h^{-1} (Fig. 5h). In addition, the concentrations of NO_3^- and NO_2^- are determined as well, which are shown in Fig. S19.

Conclusions

In conclusion, a self-powered electrocatalytic system driven by a high-output dual-TENG device is designed to synthesize ammonia, which has special advantages in reactants and electrolyte over electrocatalytic N_2 reduction. By air discharging caused by a TENG device, nitrogen is fixed into NO_X directly using air as the source for further electrolyte formation. Meanwhile, driven by the other TENG, electrocatalytic reduction using TiO_2 as the catalyst is carried out to synthesize ammonia in a dual-compartment electrocatalytic cell. Under the simulated waste gas at a flow rate of 3.5 m^3 min^{-1}, ammonia yield per hour of the self-powered electrocatalytic system is 2.4 μg h^{-1} at ambient conditions. Compared with traditional synthetic methods, the system possesses advantages of self-powered, eco-friendly, low-cost, facile-fabrication, and scalable, showing a great potential for ammonia synthesis.

Experimental Section

Fabrication of the dual-TENG

The stator is a custom-made PCB circuit with 6 pairs of Cu electrodes and fixed on an aluminum plate. A circle region with a diameter of 40 mm is cut in the center of PCB board for the space of drive shaft. The distance between each electrode is 5 mm. A custom-made FR-4 board is used as the substrate disc for the rotor. The diameter of the disc is 200 mm, and the thickness is 0.3 mm. The reserved hole on it is used to connect with the shaft. According to the electrode, the Kapton film (60 μm) is cut into a fan shape with the area of about 22 cm^2 and stuck on the disc with space. Then, two pair of stators and rotors are assembled in vertical direction with the help of PMMA baseboards to tune the height.

Measurements of the basic performance of dual-TENG

Charge and current data at different rotation speeds are measured by an electrometer (6514, Keithley Ltd.) with a LabVIEW program. Since the high voltage of TENG exceeds the range of electrometer, a multimeter with high-voltage attenuation (HVP-40, PINTEK Ltd.) is utilized. The following experiments are conducted under the condition of 5000 r min^{-1}, including air discharge and electrocatalytic reduction sections.

Fabrication of the discharge device and relevant measurements

The discharge device is simply fabricated by a common steel needle and a Tantalum sheet (2 cm x 2 cm x 0.1 mm) with a PMMA frame. To reduce the effect of reflection on pictures, a layer of black sponge is covered on the surface of PMMA. The spark discharge pictures are taken by a high-speed camera to show clear phenomenon.

The discharge device and a NO_X detector (BH-90, Bosean Ltd.) is placed in a sealed PMMA box. Volume of the box is about 1 L without the detector counted in. The box can be reopened to tune the distance between the needle and the bottom electrode. Besides, there are reserved inlet and outlet to help exhaust the residual gas in the box during the repeated test by a mini vacuum pump. The device is connected to a ten-stage multiplied circuit using capacitors of 50 nF and TENG-1. Each air discharge time is 5 min, then the NO_X concentration value is recorded.

To have a better collection of discharging gas, the device is replaced into a small PMMA box (4cm x 4cm x 4cm) which is connected to a gas-washing bottle (25 mL) with 20 mL pure water. The distance between the needle and the bottom electrode is set at 2 mm. A mini air pump is used to help supply gas source. After 6 h air discharge, volume of the solution and concentration of NO_3^- and NO_2^- are measured in turn. The needle is used as the positive and negative electrode respectively.

Preparation of TiO_2/carbon cloth

The commercial carbon cloth (WOS1009, Cetech Co., Ltd.) is cut into different sizes (1 cm x 1 cm and 2.5 cm x 2.5 cm). Typically, 10 mg commercial nano TiO_2 (P25) catalyst and 50 μL of nafion solution (5 wt%) are dispersed in 1 mL absolute ethyl alcohol by sonicating for 1 h to form a homogeneous ink. Then, a certain volume of the ink is loaded onto a piece of carbon cloth electrode (1 mg cm^{-2}) and dried under ambient condition.

Electrocatalytic reduction in a single cell

A single electrochemical cell with 60 mL volume is used to have electrocatalytic verification experiments. The anode is graphite electrode (1 cm x 1 cm x 3 mm), the cathode is naked carbon cloth or TiO_2/carbon cloth with the same size. The cyclic voltammetry curve is measured in a 20 mL of 100 mg L^{-1} NO_3^- or

NO_2^- solution with the reference of saturated calomel electrode by an electrochemical workstation (CHI 660E, CHEN HUA Ltd.) at a scan rate of 0.05 V s^{-1}. 20 mL of 100 mg L^{-1} NO_3^- and 20 mg L^{-1} NO_2^- solutions are used as electrolytes. Driven by a DC power at -3 V for 6 h, the concentration of NO_3^-, NO_2^- and target production of NH_3 are determined, respectively. Since the concentration may exceed the range of standard curve, the solution may be diluted to make determination according to the specific circumstance. When using TENG-2 as the power, a rectifier and a series of custom-made transformers are used before driving the catalytic reaction. Besides, a normal multimeter is utilized to have quick tests of the voltage and current of the electrocatalytic system.

Fabrication of the dual-compartment cell and relevant electrocatalytic reduction

A piece of TiO_2/carbon cloth (2.5 cm x 2.5 cm) is combined with a piece of pre-activated Nafion membrane (NRE-211, 3 cm x 3 cm) by a hot press process at 140 °C for 0.5 h. Then the combination is assembled with two pieces of silicone and custom-made graphite bipolar plates (4 cm x 4 cm) with groove to fabricate the dual-compartment cell. A 20 mL of pure water and a 20 mL of 100 mg L^{-1} NO_3^- solution are recycled in the anode and cathode compartment with the help of two peristaltic pumps both at a rate of 1 mL min^{-1}, and then both determined after 1 h reaction driven by TENG-2 separately.

Self-powered ammonia synthesis

A blower (STPT600-A9, STANLEY Ltd.) is used as the simulated gas source. The dual-TENG is transferred from the DC rotor platform and connected to the blower by a simple turbocharger with two turbofans. Then the discharge device and the dual-compartment cell are assembled with TENGs to synthesize ammonia. At a flow rate of 3.5 m^3 min^{-1}, the solution in the anode and cathode region are determined after 10 h reaction separately.

Conflicts of interest

There are no conflicts to declare.

Acknowledgements

The research was supported by the National Key R & D Project from the Minister of Science and Technology (2016YFA0202704), Youth Innovation Promotion Association, CAS, Beijing Municipal Science & Technology Commission (Z171100000317001, Z171100002017017, Y3993113DF), and National Natural Science Foundation of China (Grant No. 51605033, 51432005, 5151101243, 51561145021). In addition, thanks a lot for the help from Dr. Jian Chen, Yu Bai and Qingsong Lai.

References

1 S. Giddey, S. P. S. Badwal, A. Kulkarni, *Int. J. Hydrogen Energy*, 2013, **38**, 14576-14594.
2 S. L. Foster, S. I. Perez Bakovic, R. D. Duda, S. Maheshwari, R. D. Milton, S. D. Minteer, M. J. Janik, J. N. Renner, L. F. Greenlee, *Nat. Catal.*, 2018, **1**, 490-500.
3 X. Cui, C. Tang, Q. Zhang, *Adv. Energy Mater.*, 2018, **8**, 1800369.
4 N. Cao, G. Zheng, *Nano Res.*, 2018, **11**, 2992-3008.
5 M.-M. Shi, D. Bao, B.-R. Wulan, Y.-H. Li, Y.-F. Zhang, J.-M. Yan, Q. Jiang, *Adv. Mater.*, 2017, **29**, 1606550.
6 L. Zhang, L.-X. Ding, G.-F. Chen, X. Yang, H. Wang, *Angew. Chem. Int. Ed.*, **58**, 2612-2616.
7 X. Li, T. Li, Y. Ma, Q. Wei, W. Qiu, H. Guo, X. Shi, P. Zhang, A. M. Asiri, L. Chen, B. Tang, X. Sun, *Adv. Energy Mater.*, 2018, **8**, 1801357.
8 S. Z. Andersen, V. Čolić, S. Yang, J. A. Schwalbe, A. C. Nielander, J. M. McEnaney, K. Enemark-Rasmussen, J. G. Baker, A. R. Singh, B. A. Rohr, M. J. Statt, S. J. Blair, S. Mezzavilla, J. Kibsgaard, P. C. K. Vesborg, M. Cargnello, S. F. Bent, T. F. Jaramillo, I. E. L. Stephens, J. K. Nørskov, I. Chorkendorff, *Nature*, 2019, **570**, 504-508.
9 B. H. R. Suryanto, H.-L. Du, D. Wang, J. Chen, A. N. Simonov, D. R. MacFarlane, *Nat. Catal.*, 2019, **2**, 290-296.
10 C. Tang, S.-Z. Qiao, *Chem. Soc. Rev.*, 2019, **48**, 3166-3180.
11 F. Zhou, L. M. Azofra, M. Ali, M. Kar, A. N. Simonov, C. McDonnell-Worth, C. Sun, X. Zhang, D. R. MacFarlane, *Energy Environ. Sci.*, 2017, **10**, 2516.
12 Z. Sun, R. Huo, C. Choi, S. Hong, T.-S. Wu, J. Qiu, C. Yan, Z. Han, Y. Liu, Y.-L. Soo, Y. Jung, *Nano Energy*, 2019, **62**, 869-875.
13 Y. Wang, A. Xu, Z. Wang, L. Huang, J. Li, F. Li, J. Wicks, M. Luo, D.-H. Nam, C.-S. Tan, Y. Ding, J. Wu, Y. Lum, C.-T. Dinh, D. Sinton, G. Zheng, E. H. Sargent, *J. Am. Chem. Soc.*, 2020, **142**, 5702-5708.
14 Y. Wang, W. Zhou, R. Jia, Y. Yu, Bin Zhang, *Angew. Chem. Int. Ed.*, 2020, **59**, 5350-5354.
15 F.-R. Fan, Z.-Q. Tian, Z. L. Wang, *Nano Energy*, 2012, **1**, 328-334.
16 Z. L. Wang, *Mater. Today*, 2017, **20**, 74-82.
17 S. Niu, Z. L. Wang. *Nano Energy*, 2015, **14**, 161-192.
18 C. Wu, A. C. Wang, W. Ding, H. Guo, Z. L. Wang, *Adv. Energy Mater.*, 2019, **9**, 1802906
19 W. Tang, C. Zhang, C. B. Han, Z. L. Wang, *Adv. Funct. Mater.*, 2014, **24**, 6684-6690.
20 G. Zhu, P. Bai, J. Chen, Q. Jing, Z. L. Wang, *Nano Energy*, 2015, **14**, 126-138.
21 W. Tang, T. Jiang, F. R. Fan, A. F. Yu, C. Zhang, X. Cao, Z. L. Wang, *Adv. Funct. Mater.*, 2015, **25**, 3718-3725.
22 Z. L. Wang, T. Jiang, L. Xu, *Nano Energy* 2017, **39**, 9-23.
23 X.-S. Zhang, M. Han, B. Kim, J.-F. Bao, J. Brugger, H. Zhang, *Nano Energy*, 2018, **47**, 410-426.
24 H. R. Zhu, W. Tang, C. Z. Gao, Y. Han, T. Li, X. Cao, Z. L. Wang, *Nano Energy*, 2015, **14**, 193-200.
25 Y. Feng, K. Han, T. Jiang, Z. Bian, X. Liang, X. Cao, H. Li, Z. L. Wang, *Nano Res.*, 2019, **12**, 2729-2735.
26 K. Han, J. Luo, Y. Feng, Q. Lai, Y. Bai, W. Tang, Z. L. Wang, *ACS Nano*, *ACS Nano*, 2020, **14,** 2751-2759.
27 K. Zhao, G. Gu, Y. Zhang, B. Zhang, F. Yang, L. Zhao, M. Zheng, G. Cheng, Z. Du, *Nano Energy*, 2018, **53**, 898-905.
28 M.-C. Wong, W. Xu, J. Hao, *Adv. Funct. Mater.*, 2019, **29**, 1904090.
29 S. Bilgen, *Renewable Sustainable Energy Rev.*, 2014, **38**, 890-902.
30 R. Bálek, S. Pekárek, *Plasma Sources Sci. Technol.*, 2018, **27**, 075019.
31 N. Rehbein, V. Cooray, *J. Electrost.* 2001, **51-52**, 333-339.
32 J. Cheng, W. Ding, Y. Zi, Y. Lu, L. Ji, F. Liu, C. Wu, Z. L. Wang, *Nat. Commun.*, 2018, **9**, 3733.
33 W. Liu, Z. Wang, G. Wang, G. Liu, J. Chen, X. Pu, Y. Xi, X. Wang, H. Guo, C. Hu, Z. L. Wang, *Nat. Commun.*, 2019, **10**, 1426.

View Article Online
DOI: 10.1039/D0EE01102A

34 Z. Wang, W. Liu, J. Hu, W. He, H. Yang, C. Ling, Y. Xi, X. Wang, A. Liu, C. Hu, *Nano Energy*, 2020, **69**, 104452.
35 Y. P. Raizer, Gas Discharge Physics, Springer, Berlin, 1991, 324-375.
36 A. Pandikumar, S. Manonmani, R. Ramaraj, *Catal. Sci. Technol.*, 2012, **2**, 345-353.
37 D. E. Kim, D. Pak, *Chemosphere* 2019, **228**, 611-618.
38 J. Gao, B. Jiang, C. Ni, Y. Qi, Y. Zhang, N. Oturan, M. A. Oturan, *Appl. Catal., B* 2019, **254**, 391-402.
39 D. Saravanakumar, J. Song, S. Lee, N. Hur, W. Shin, *ChemSusChem*, 2017, **10**, 3999-4003.

View Article Online
DOI: 10.1039/D0EE01102A

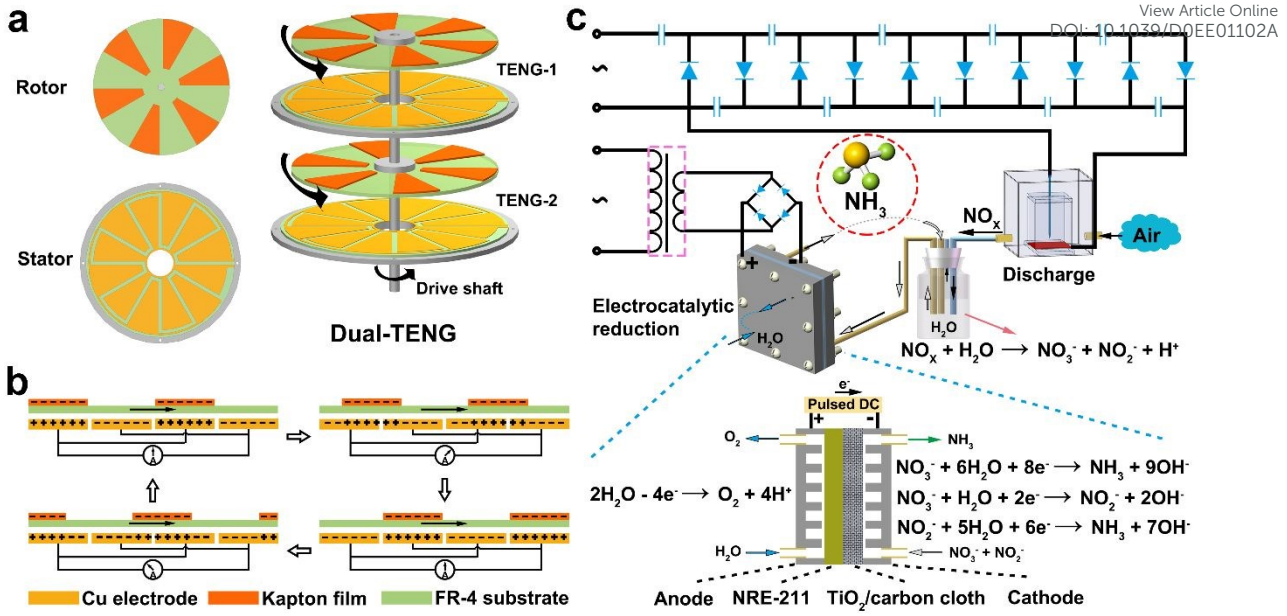

Fig. 1 Schematic diagram. (a) Construction of the dual-TENG device. (b) Working principle of the TENG. (c) Ammonia synthesis devicess, main reaction processes and mechanism.

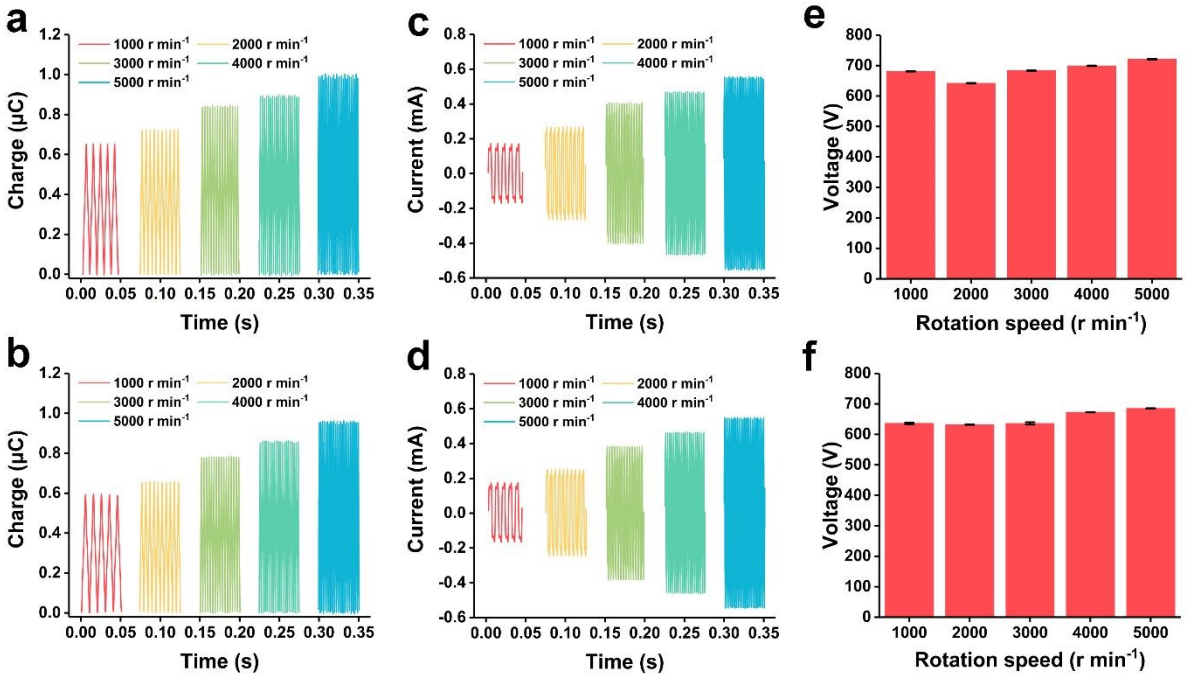

Fig. 2 (a) Transferred charge of TENG-1. (b) Transferred charge of TENG-2. (c) Short-circuit current of TENG-1. (d) Short-circuit current of TENG-2. (e) Open-circuit Voltage of TENG-1. (f) Open-circuit Voltage of TENG-2.

View Article Online
DOI: 10.1039/D0EE01102A

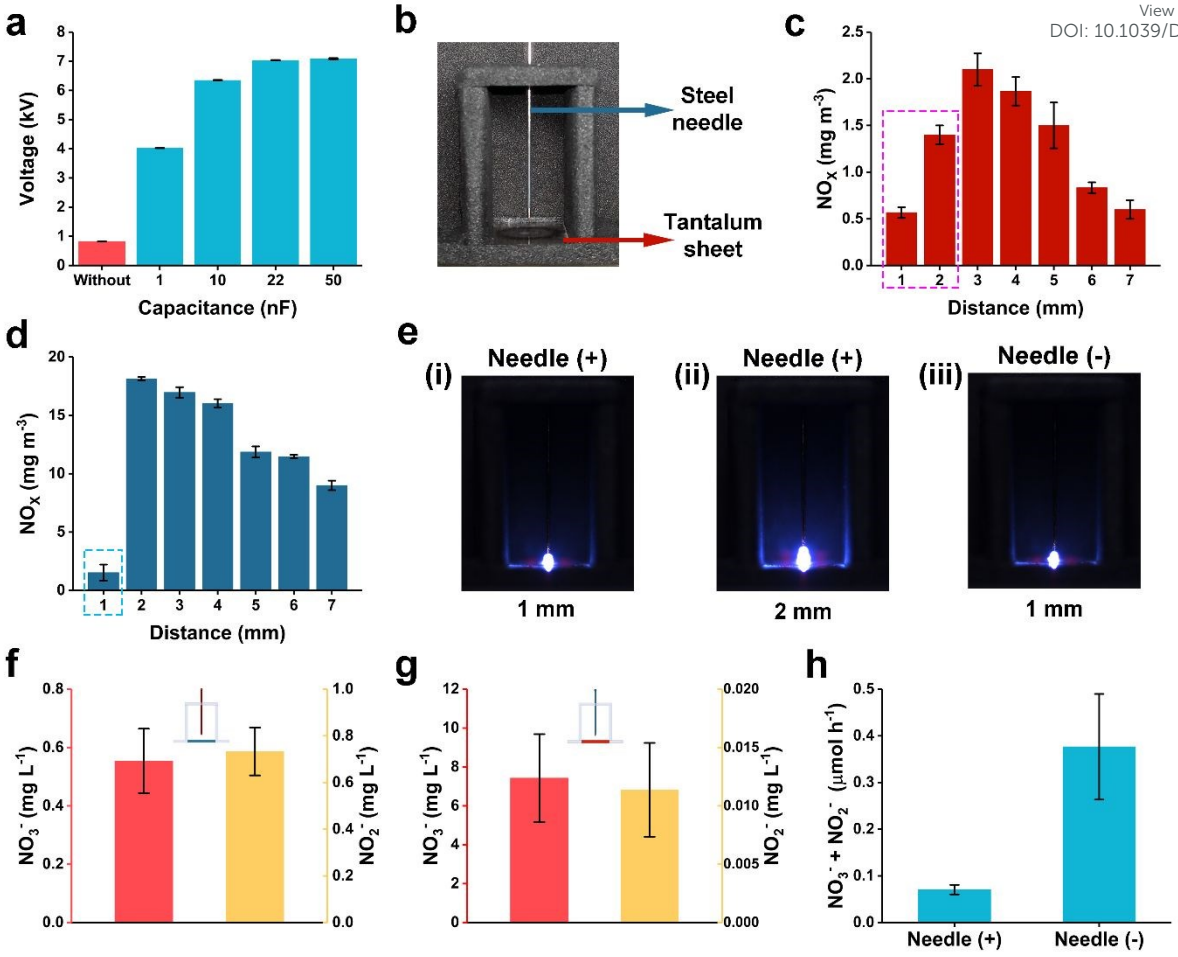

Fig. 3 (a) Voltage variation of TENG-1 using ten-stage voltage multiplier circuits with different capacitors. (b) Pictures of the air discharge device. Concentrations of NO_X using needle (c) as the positive electrode and (d) as the negative electrode after 5 min discharge in a sealed box. (e) Typical pictures of spark discharge at different conditions. Concentrations of NO_3^- and NO_2^- using needle (f) as the positive electrode and (g) as the negative electrode after air discharges and passes through a 20 ml of pure water for 6 h. (h) Comparison of total water soluble ions containing nitrogen in mole yield per hour.

View Article Online
DOI: 10.1039/D0EE01102A

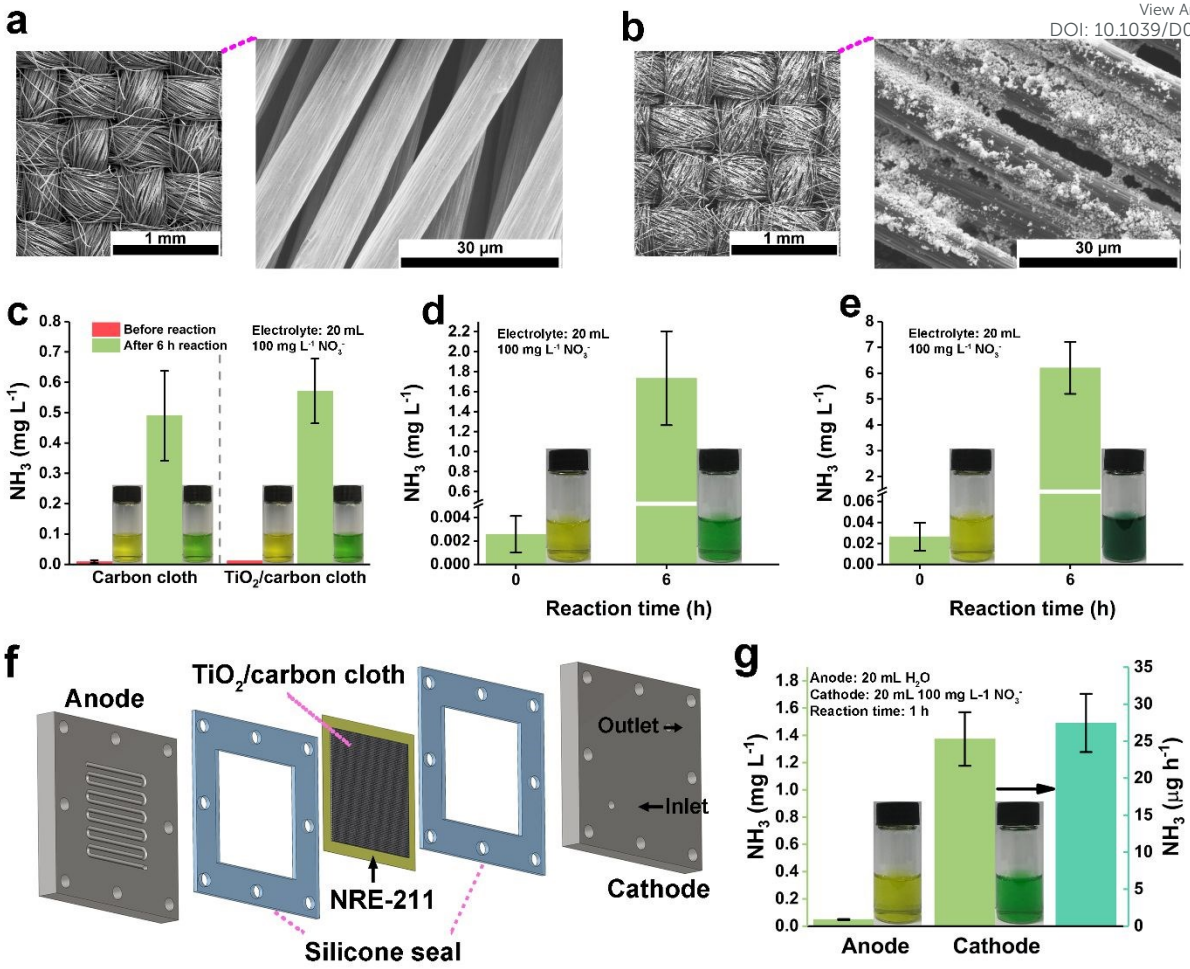

Fig. 4 (a) SEM images of carbon cloth. (b) SEM images of TiO_2/carbon cloth. Concentration variations of NH_3 using 100 mg L^{-1} NO_3^- as electrolyte in a single cell with (c) a DC power (-3V) drive, (d) rectified TENG-2 drive and (e) voltage step-down (350:12) and rectified TENG-2 drive. (f) Construction of the dual-compartment electrocatalytic cell with a fuel cell structure. (g) Concentration and mass yield per hour of NH_3 in a dual-compartment electrochemical cell with voltage step-down (350:4) and rectified TENG-2 drive.

View Article Online
DOI: 10.1039/D0EE01102A

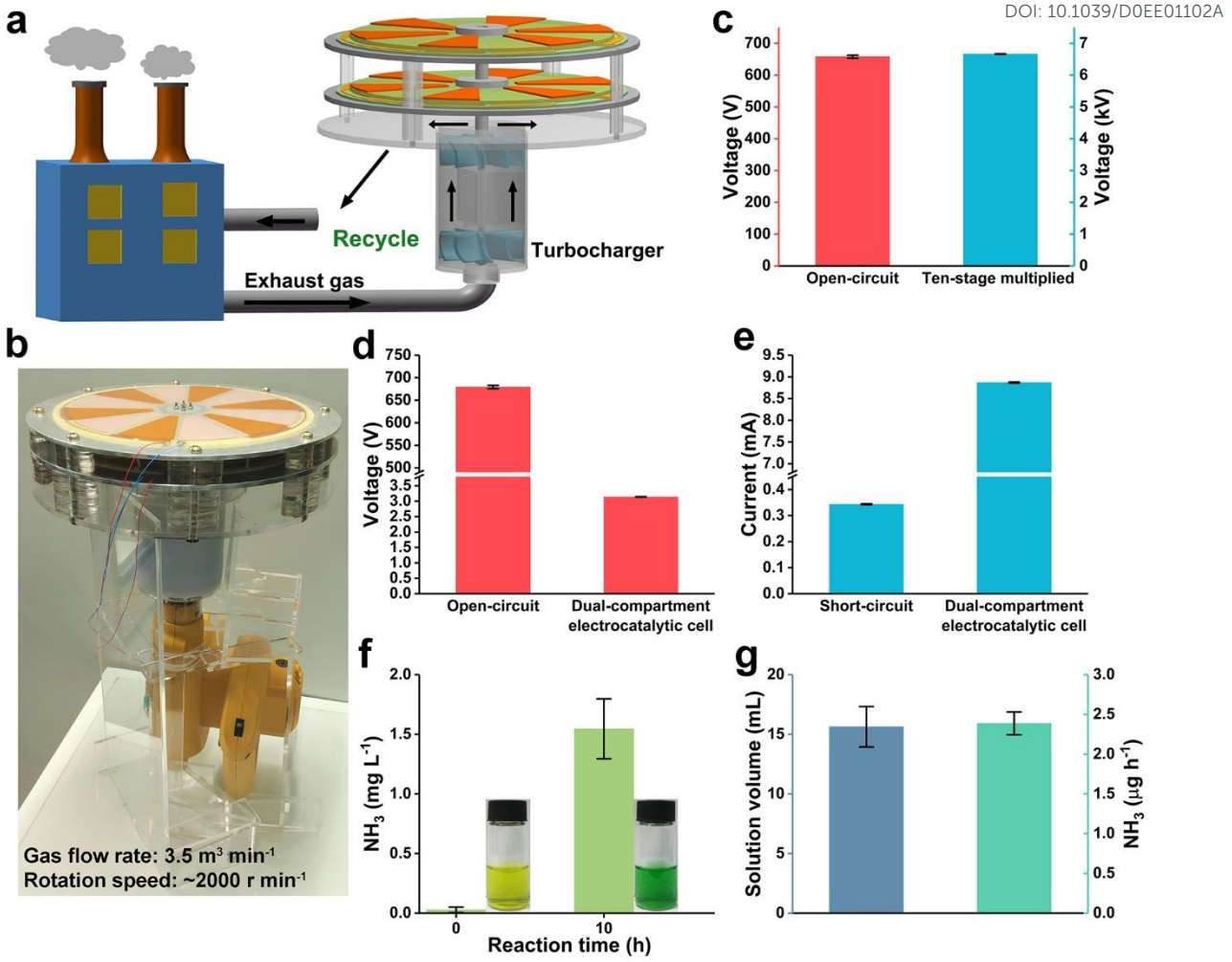

Fig. 5 (a) Schematic diagram of the self-powered dual-TENG device. (b) Picture of the self-powered dual-TENG device with a blower as the simulated exhaust gas source. (c) Open-circuit voltage and ten-stage multiplied voltage of TENG-1. (d) Open-circuit voltage of TENG-2 and voltage of the dual-compartment electrocatalytic cell with voltage step-down (350:5) and rectified TENG-2 drive. (e) Short-circuit current of TENG-2 and current of the dual-compartment electrocatalytic cell with voltage step-down (350:5) and rectified TENG-2 drive. (f) Concentration of NH_3 in the cathode compartment by self-powered synthesis for 10 h. (g) Residual solution volume in the cathode compartment and production per hour of NH_3 by self-powered synthesis for 10 h.

View Article Online
DOI: 10.1039/D0EE01102A

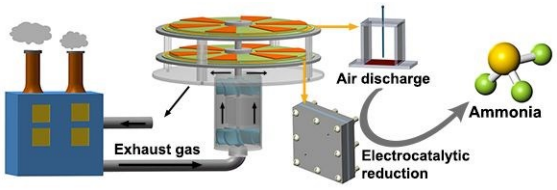

Driven by dual triboelectric nanogenerators, the nitrogen fixation from air and electrocatalytic reduction can proceed simultaneously for self-powered ammonia synthesis.

The high demand for ammonia as one of the largest inorganic production in the world, has led to a huge consumption of energy and plenty of relevant environmental pollution problems, which are great pressure to our society. It is urgent to develop energy-saving and eco-friendly methods for ammonia synthesis. By introducing a high-output dual triboelectric nanogenerator (TENG) configuration, a self-powered electrocatalytic ammonia synthesis system was constructed to achieve this. In this system, the whole synthetic process can proceed under ambient conditions. Instead of high purity N_2 requirement in other methods, air can be directly used as nitrogen source by simple discharging caused by one TENG. Then, the fixation product is utilized to form the electrolyte solution for the synchronous electrocatalytic synthesis of ammonia driven by the other TENG with a non-noble-metal catalyst involved in. Furthermore, with the help of a turbocharger, it is feasible to reuse the residual kinetic energy of exhaust gas from factories to drive the ammonia synthesis system. Compared with traditional synthetic methods, this system possesses advantages of self-powered, eco-friendly, low-cost, facile-fabrication, and scalable, showing a great potential for ammonia synthesis.